

# Phase Diagram and Snap-Off Transition for a Twisted Balloon

Yu-Chuan Cheng<sup>1</sup>, Jih-Chiang Tsai<sup>2</sup>, and Tzay-Ming Hong<sup>1,\*</sup>

<sup>1</sup>*Department of Physics, National Tsing Hua University, Hsinchu, Taiwan 30013, Republic of China*

<sup>2</sup>*Institute of Physics, Academia Sinica, Taipei, Taiwan 11529, Republic of China*

(Dated: October 20, 2020)

Turning balloons into dogs, swords, flowers, and crowns by twisting is a common childhood memory for all of us. Snapping the balloon into two separate compartments is a necessary step that bears resemblance to the pinch-off phenomenon of a droplet about to be detached from the faucet. In addition to testing whether balloons exhibit the properties of self-similarity, finite-time singularity, and memory effect that are often associated with the latter event, we determine the phase diagram for the balloon configurations by experiments. It mainly consists of six different shapes, namely, straight, necking, wrinkled, snapping, helix, and supercoil, depending on the twisting angle and the ratio of length and radius. Heuristic models are provided to explain and obtain analytic forms for the phase boundaries. Finally, we discuss and compare the results with other twisted systems, such as a cylindrical shell, ribbon, thread, and tendril.

Twisting and bending elastic filaments or ribbons [1] has fascinated scientists for centuries, such as a coil formed by twisting a rope [2] and tendril of the climbing plant [3]. In recent years, due to the progress of biology, research on DNA and protein structures and functions makes this topic popular again [4]. For a long rod or wire, a one-dimensional description suffices since the thickness is much smaller than the length. In this Letter, we investigate the twisting of an inflated party balloon, as in Fig. 1(a), for which the rubber thickness  $t$  is replaced by radius  $R$  that is comparable to length  $L$ . As a result, the balloon geometry should be viewed as being intermediate between a 1-D rod [5] and a 2-D ribbon [6].

Balloon is an example of soft material that is easily accessible and fun to play with. When inflated with air or fluid, it exhibits many interesting phenomena, such as a longitudinal phase separation during inflating [7], deformation and bursting when it impacts a rigid wall [8], fragmentation due to bursting [9], and air transfer between two balloons [10]. The initial goal of this work is more mundane, i.e., we want to know how many configurations can a twisted balloon exhibit besides snapping. Over time, we are intrigued by the similarity between how a balloon snaps and the pinch-off process that occurs in water dripping from a faucet [11, 12], bubble formation [13, 14], elephant trunks of interstellar gas and dust in the Eagle Nebula [15], and the sticky “capture blob” used by *Bolas spider* [16].

As shown in Fig.1(b), our experimental setup consists mainly of two parts, a frictionless rail and a force sensor. The former is composed of two hollow coaxial cylinders, A and B, through which the balloon is inserted. The inner diameter of the cylinders is adjustable. The cylinder A is the active side via which we twist the balloon around a bearing fixed on a desk. In the mean time, the combination of wires of length  $W = 2\text{m}$  and sliding rails that are fixed on the ceiling ensures that the cylinder B moves passively along the central axis as long as  $\Delta x < 0.05W\sin\alpha$ . While the weight prevents it from rotating with A, the cylinder B is carefully balanced by a long hollow aluminum pipe of length  $S_E$  which in turn

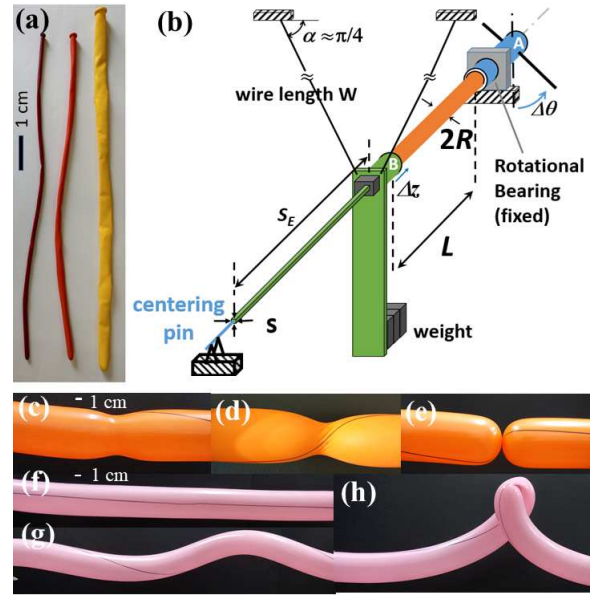


FIG. 1: (a) Samples of our uninflated balloon. (b) Schematics of experimental setup. Phases adopted by a medium-sized balloon with  $(L, R) = (160, 22)\text{mm}$  include (c) straight, (d) necking, (e) wrinkled, and (f) snapping. In contrast, a long balloon with  $(L, R) = (530, 22)\text{mm}$  exhibits (g) straight, (e) helix, and (f) supercoil.

is kept stationary by an iron centering pin. The tilt of balloon during twisting is negligible since  $s \ll S_E$ . While the stepping motor rotates at a steady angular velocity, the twist force is measured by the tension meter.

To understand why phase 1 is followed by phase 2, we need to understand why the balloon would voluntarily create a concave region which will raise its surface tension energy. By use of the relation  $\frac{F}{2r(x)t} = S \frac{r(x)d\theta}{dx}$  for shearing in elasticity, we can rewrite the constant torque in static equilibrium as

$$2\pi St \frac{r^3(x)}{\sqrt{1 + (dr/dx)^2}} \frac{d\theta}{dx} = \text{const.} \quad (1)$$

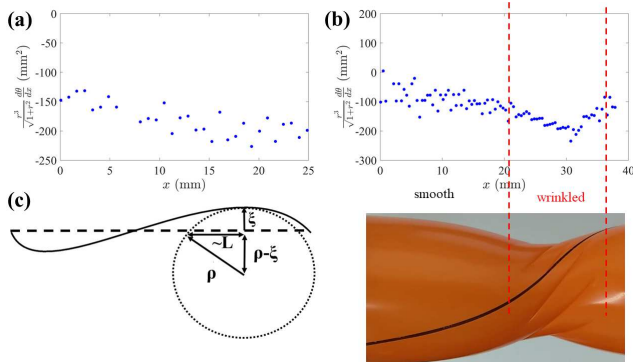


FIG. 2: The quantity in Eq. (1) is verified to be a constant of the axial position,  $x$  for regions that are wrinkle-free, e.g., the whole balloon for phase 2 in (a) and part of phase 3 in (b). Schematic plot (c) is for phase 5 where  $\xi$  denotes the radius of helix.

This conserved quantity is nicely verified in Fig. 2 (a) and (b) for the smooth region of balloon. The  $r^3$  factor in Eq. (1) implies us that by lowering  $r$ , take the limiting case of  $r \rightarrow 0$  for phase 3 for instance, can dramatically redirect almost all shear angle into the concave region.

In the following, we refer short balloons to those with  $L/R \leq 5$ . As twisting progresses, the configuration of balloon changes continuously from being (1) straight and smooth to (2) concave and smooth and (3) concaved and wrinkled. Upon reaching the final phase (4) snap-off, the transition becomes abrupt and the balloon suddenly loses its resisting torque, as evidenced by Fig. 3(a). The torque  $\tau$  increases linearly with  $\theta$  in phases (1) and (2), but bends over in phase (3) before hitting zero at (4). This mechanical response is reminiscent of that for a twisted cylindrical paper or metal shell [18], except for the absence of phases (2) and (4). Another difference is that, instead of spanning the whole  $L$ , the concaveness in balloons affects only a region about  $5R$  in length initially when  $L > 5R$ . This value is independent of  $L$  and will shrink as  $\theta$  increases. In contrast, phase (3) ceases to exist in Fig. 3(b) for a medium-sized balloon with  $5 < L/R \leq 30$ , and  $\tau$  drops precipitously to zero after reaching its peak. When the balloon is long with  $L/R > 30$ , Fig. 3(c) appears to be a repetition of (b) ostensibly, but in fact the underlying mechanism is very different. The configurations associated with phases (2~4) are replaced by (5) helix and (6) supercoil. The torque always plummets discontinuously, but the extent of drop decreases, when a new supercoil appears. This is accompanied by a larger slope in its buildup to the next supercoil due to the shortening of balloon length that is not affected by the supercoil(s).

In order to determine the phase boundaries in Fig. 3(d), we need to write down the potential energy characteristic to all phases. Shear energy for phase 1 is the simplest:

$$E_1 \sim \frac{SR^3t}{L}\theta^2 \quad (2)$$

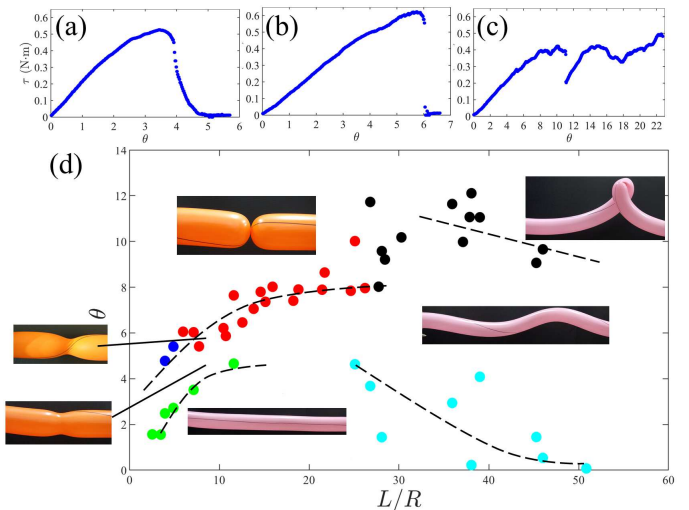


FIG. 3: (a) Phase diagram for a twisted balloon in the parameter space of  $\theta$  and  $L/R$ . Plots (b~d) shows the torque response for a short, medium, and long balloon, respectively.

where  $S$  denotes the shearing modulus. Whileas, two new rubber surfaces are created in the vicinity of necking when a balloon snaps. So for phase 2,

$$E_2 \sim TR^2 \quad (3)$$

where  $T$  is the surface tension coefficient. Phase 5 is a little bit trickier since it relieves part of the shear energy by angle  $\eta$  by distorting itself into a helix:

$$E_5 \sim \frac{SR^3t}{L}(\theta - \eta)^2 + K_b\left(\frac{1}{\rho}\right)^2RL \quad (4)$$

where the curvature  $1/\rho \sim \eta/L$  can be obtained from the Pythagorean theorem as shown in Fig. 2(c),  $\rho^2 = (\rho - \xi)^2 + L^2$ , that requires  $\rho \sim L^2/\xi$ . The fact that  $\xi$  is linked to  $\eta$  by  $\xi \sim \eta L$  immediately leads to  $\rho \sim L/\eta$ .

Now we are set to pinpoint the phase boundary. Equating Eqs.(2) and (3) identifies the borderline between phases 1 and 2 at  $\theta_{1,2} \approx \sqrt{L/R}$ . By setting the angle  $\eta$  that minimizes  $E_5$  at  $2\pi$ , we can locate the dividing line between phases 5 and 6 at

$$\theta_{5,6} \approx 2\pi + \frac{Y}{S}, \quad (5)$$

independent of  $L, R$  and  $K_b \sim YR^2t$  from elasticity [19] has been used. The same conclusion has been derived [20] for a twisted filament, which is not surprising because Eq. 5 remains valid when we set  $t = R$  to simulate the filament. Note that  $\theta_{5,6}$  decreases slightly with  $L$ . We believe it is due to the fact that the elongation of balloon has far exceeded the yield strain.

Experience tells us that the snapping of a balloon is abrupt and voluntary. In other words, like the bursting of soap bubble, we expect the configuration of short and medium-sized balloons transits from being reversible to

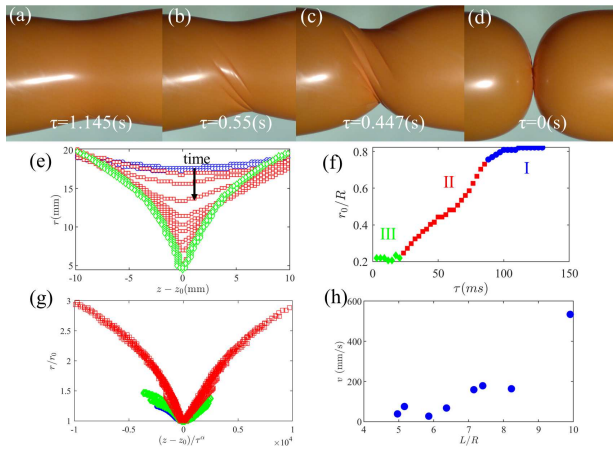


FIG. 4: (a~d) Photos of configurational change for a balloon with  $L/R = 7.3$  leading up to the snap. (e) Time evolution of balloon profile where  $z_0$  is the position at the bottle neck that shifts with  $\theta$ . To facilitate comparison we set the  $x$ -axis parameter as  $z - z_0$ . Three regimes are respectively denoted by circles, squares, and diamonds. Plot (f) is  $r_0$  vs  $\tau$ . (g) Data points in regime II can be made to collapse to a master curve by rescaling with  $\alpha = 2$ . (h) Shrinking velocity for regime II increases with  $L/R$ .

irreversible beyond  $\theta_{3,4}$ . A high-speed camera with 8000 fps captures the dynamical process that leads up to the singular neck. Photos in Fig. 4(a) and (b) belong to the reversible regime I and correspond to phase 2 and 3. We observed that the ordering of wrinkles suddenly improves when the balloon enters the irreversible regime where Fig. 4 (c) and (d) belong to phase 3 and 4, respectively. This distinction is based on whether their profile, mapped out by photo detection in Fig. 4(e), is smooth or exhibits a singular point. Further evidence comes from Fig. 4(f) that shows the shrinking velocity transits from being constant to decelerating as  $\propto \tau^{-8/5}$  where  $\tau \equiv t_0 - t$ . Self-similarity, often associated with the pinch-off phenomenon, means that the profiles of droplet at successive times can be mapped to a master curve if we rescale the length and count-down time[12]. This is checked in Fig. 4(g). We do not yet understand why  $\alpha = 2$ , as opposed to the usual value of 1 for Stokes flow[29]. It is worth noting that the velocity in regime II varies with  $L/R$  according to Fig. 4(h). This is un-

usual because during the typical process of liquid pinch-off the shrinking velocity only depends on the flow of inner liquid [17] and is insensitive to initial conditions.

If the interior viscosity is sufficiently small, as it is for an air bubble in thick syrup, the zero-viscosity drop breakup dynamics persist down to the atomic scales. However, if the interior viscosity is large enough, or the exterior viscosity small enough, the singularity will be cut off.

Besides self-similarity and memory effect [17], finite-time singularity [23] is often addressed that requires  $r \propto \tau^\beta$  to obey a power-law relation. These properties are compiled in Table I for selective pinch-off systems to highlight the uniqueness of twisted balloon - rescaling exponent  $\alpha$  being greater than 1 and the dependence on initial condition. As is listed in the first column, regime II is characterized by the balance of two dominant driving forces, surface tension and the effect of inertia or/and viscosity. How about the shear energy? It only enters in regime III and disrupts the aforementioned balance which we believe is why the shrinking velocity ceases to remain a constant. How do we know that? A clue came from observing the marking we drew on the balloon before twisting, as shown in Fig. 1 (c-e). The wrinkles in Fig. 4(c) appears to create an energy barrier that hinders the relaxation of shear energy, as evidence by the fact that the marking remains tilted in regime II. According to Eq. (1), the tendency to relocate the twist or shear strain to the necking increases with decreasing  $r$ . Presumably this is why the marking finally reverts to nearly horizontal by a sudden click upon entering regime III.

In summary, we show that the usual party balloon can exhibit six different configurations when twisted, depending on the twist angle and aspect ratio between length and radius. Phase diagram is determined experimentally whose boundaries can be consistently derived by comparing the potential energy that correspond to different phases. Special attentions are paid to clarify the analogy between the snapping process and the well-studied pinch-off phenomenon in fluid dynamics. Unlike the latter, the shrinking velocity of balloon is sensitive to the initial condition - its length.

We gratefully acknowledge technical assistance from Wei-Chi Lee and Hsin-Hu Li and financial support from MoST in Taiwan under Grants No. 105-2112-M007-008-MY3 and No. 108-2112-M007-011-MY3.

\* ming@phys.nthu.edu.tw

- [1] Yasuaki Morigaki, Hirofumi Wada, and Yoshimi Tanaka, Stretching an Elastic Loop: Crease, Helicoid, and Pop Out, *Phys. Rev. Lett.* **117**, 198003 (2016).
- [2] A. Ghatak and L. Mahadevan, Solenoids and Plectonemes in Stretched and Twisted Elastomeric Filaments, *Phys. Rev. Lett.* **95**, 057801 (2005).
- [3] S. J. Gerbode, J. R. Puzey, A. G. McCormick, and L. Mahadevan, How the cucumber tendrils coils and overwinds,

*Science* **337**, 1087 (2012).

- [4] Andrew Dittmore, Sumitabha Brahmachari, Yasuharu Takagi, John F. Marko, and Keir C. Neuman, Supercoiling DNA Locates Mismatches, *Phys. Rev. Lett.* **119**, 147801 (2017).
- [5] Nicholas Charles, Mattia Gazzola, and L. Mahadevan, Helicoids, Topology, Geometry, and Mechanics of Strongly Stretched and Twisted Filaments: Solenoids, Plectonemes, and Artificial Muscle Fibers, *Phys. Rev.*

TABLE I: Comparing properties, with the first four for regime II and the fifth one for III, for selective systems exhibiting the pinch-off where S, I, V, and D represent surface tension, inertia, viscosity, and diffusion, and Y/N the shorthand for yes/no.

	dominant terms	self-similarity		memory effect	satellite bubble
		$\alpha$	$\beta$		
twisting balloon	S and I	1	1	Y	N
bubble in capillary tube <sup>a</sup>	S and V	1 and 1	1/5 and 1/2	N	N
volume-conserved bubble <sup>b</sup>	S and I	1 and 2/3	1 and 2/3	N	Y
droplet in silicon oil <sup>c</sup>	S and V	1	1	Y/N	Y
ultra-low surface tension <sup>d</sup>	D and V	1/3	1/3	N	N
Bubble in turbulence <sup>e</sup>	S and I	1/2	X	N	Y

<sup>a</sup>Reference [31]

<sup>b</sup>Reference [26]

<sup>c</sup>Reference [12, 21–25]

<sup>d</sup>Reference [30]

<sup>e</sup>Reference [27]

- Lett. **123**, 208003 (2019).
- [6] Julien Chopin and Arshad Kudrolli, Helicoids, Wrinkles, and Loops in Twisted Ribbons, *Phys. Rev. Lett.* **111**, 174302 (2013).
- [7] Andrea Giudici and John S. Biggins, Ballooning, bulging, and necking: An exact solution for longitudinal phase separation in elastic systems near a critical point, *Phys. Rev. E* **102**, 033007 (2020).
- [8] Etienne Jambon-Puillet, Trevor J. Jones and P.-T. Brun, Deformation and bursting of elastic capsules impacting a rigid wall, *Nat. Phys.* **16**, 585 (2020).
- [9] Sébastien Moulinet and Mokhtar Adda-Bedia, Popping Balloons: A Case Study of Dynamical Fragmentation, *Phys. Rev. Lett.* **115**, 184301 (2015).
- [10] Yan Levin and Fernando L. da Silveira, Two rubber balloons: Phase diagram of air transfer, *Phys. Rev. E* **69**, 051108 (2004).
- [11] Pankaj Doshi and Osman A. Basaran, Self-similar pinch-off of power law fluids, *Phys. Fluids* **16**, 585 (2004).
- [12] I. Cohen, M. P. Brenner, J. Eggers, and S. R. Nagel, Two Fluid Drop Snap-Off Problem: Experiments and Theory, *Phys. Rev. Lett.* **83**, 1147 (1999).
- [13] J. Erlebacher, Mechanism of Coarsening and Bubble Formation in High-Genus Nanoporous Metals, *Phys. Rev. Lett.* **106**, 225504 (2011).
- [14] Louis Salkin, Alexandre Schmit, Pascal Panizza, and Laurent Courbin, Generating Soap Bubbles by Blowing on Soap Films, *Phys. Rev. Lett.* **116**, 077801 (2016).
- [15] [https://en.wikipedia.org/wiki/Pillars\\_of\\_Creation](https://en.wikipedia.org/wiki/Pillars_of_Creation).
- [16] [https://en.wikipedia.org/wiki/Bolas\\_spider](https://en.wikipedia.org/wiki/Bolas_spider).
- [17] X. D. Shi, Michael P. Brenner, Sidney R. Nagel, A Cascade of Structure in a Drop Falling from a Faucet, *Science* **265**, 219 (1994).
- [18] L. M. Wang, S. T. Tsai, C. Y. Lee, P. Y. Hsiao, J. W. Deng, H. C. Fan Chiang, Y. Fei, and T. M. Hong, Crumpling-origami transition for twisting cylindrical shells, *Phys. Rev. E* **101**, 053001 (2020).
- [19] See Supplemental Material at \*\*\* for detailed calculations.
- [20] A. Goriely and M. Tabor, The Nonlinear Dynamics of Filaments. *Nonlinear Dynamics* **21**, 101 (2000).
- [21] J. Eggers, Universal Pinching of 3D Axisymmetric FreeSurface Flow, *Phys. Rev. Lett.* **71**, 3458 (1993).
- [22] W. W. Zhang and J. R. Lister, Similarity Solutions for Capillary Pinch-Off in Fluids of Differing Viscosity, *Phys. Rev. Lett.* **83**, 1151 (1999).
- [23] J. R. Lister and H. A. Stone, Capillary breakup of a viscous thread surrounded by another viscous fluid, *Phys. Fluids* **10**, 2758 (1998).
- [24] A. S. Utada, A. Fernandez-Nieves, H. A. Stone, and D. A. Weitz, Dripping to Jetting Transitions in Coflowing Liquid Streams, *Phys. Rev. Lett.* **99**, 094502 (2007).
- [25] M. Rubio, A. Ponce-Torres, E. J. Vega, M. A. Herrada, and J. M. Montanero, Complex behavior very close to the pinching of a liquid free surface, *Phys. Rev. Fluids* **4**, 021602 (2019).
- [26] W. Z. Li, C. Y. Shih, T. L. Chang and T. M. Hong (unpublished).
- [27] Daniel J. Ruth, Wouter Mostert, Stéphane Perrard, and Luc Deike, Bubble pinch-off in turbulence, *Proc. Natl. Acad. Sci. U.S.A.* **116**, 25412 (2019)
- [28] L. K. Aagesen, A. E. Johnson, J. L. Fife, P. W. Voorhees, M. J. Miksis, S. O. Poulsen, E. M. Lauridsen, F. Marone, and M. Stampanoni, Universality and self-similarity in pinch-off of rods by bulk diffusion, *Nat. Phys.* **6**, 796 (2010).
- [29] John R. Lister and Howard A. Stone, Capillary breakup of a viscous thread surrounded by another viscous fluid, *Phys. Fluids* **10**, 2758 (1998)
- [30] Hau Yung Lo, Yuan Liu, Sze Yi Mak, Zhuo Xu, Youchuang Chao, Kaye Jiale Li, Ho Cheung Shum, and Lei Xu, Diffusion-Dominated Pinch-Off of Ultralow Surface Tension Fluids, *Phys. Rev. Lett.* **123**, 134501 (2019)
- [31] A. A. Pahlavan, H. A. Stone, G. H. McKinley, and R. Juanes, Restoring universality to the pinch-off of a bubble, *Proc. Natl. Acad. Sci. U.S.A.* **116**, 13780 (2019)